Stanislav KITAROVIĆ
Vedran ŽANIĆ
Jerolim ANDRIĆ

Progressive Collapse Analyses of Stiffened Box- Girders Submitted to Pure Bending

Authors' address:
University of Zagreb, Faculty of Mechanical Engineering and Naval Architecture,
I. Lučića 5, 10000 Zagreb, Croatia; E-mail: stanislav.kitarovic@fsb.hr

Original scientific paper

Two of the most distinctive contemporary approaches for determination of the ultimate bending load capacity of the stiffened thin-walled structures are: geometrically and materially nonlinear finite element method and various incremental-iterative methods based on Smith's approach. While the nonlinear finite element analysis method can be considered as the most comprehensive and potentially the most accurate available approach, the methods based on Smith's approach are prescribed by many classification societies (and their associations) and can be considered as the most widespread and most utilized among currently employed progressive collapse analysis methods. Results obtained by both methods are benchmarked against the results of experimental testing of various stiffened box girders submitted to extreme pure bending. Within context of the considered problem, the influence of various relevant aspects of the employed methods is evaluated and critically discussed, considering both levels (global and local) of structural response.

Keywords: *nonlinear finite element method, progressive collapse analysis, Smith's method, stiffened box girder, ultimate load-capacity, ultimate strength*

Analize progresivnog kolapsa tankostjenih kutijastih nosača opterećenih čistim savijanjem

Izvorni znanstveni rad

Među trenutno najznačajnijim pristupima određivanju graničnog savojnog opterećenja ukrepljenih tankostjenih konstrukcija najviše se ističu: geometrijski i materijalno nelinearna metoda konačnih elemenata i različite inkrementalno-iterativne metode zasnovane na Smithovom pristupu. Dok se analiza nelinearnom metodom konačnih elemenata može smatrati najsveobuhvatnijim i potencijalno najtočnijim raspoloživim pristupom, primjenu metoda zasnovanih na Smithovom pristupu propisuju pravila mnogih klasifikacijskih društava (i njihovih asocijacija) te su najrasprostranjenije i najzastupljenije među trenutno korištenim metodama analize progresivnog kolapsa. Rezultati obiju metoda uspoređeni su s rezultatima eksperimentalnog ispitivanja različitih ukrepljenih kutijastih nosača opterećenih ekstremnim čistim savijanjem. U kontekstu razmatranog problema razmotren je i kritički prodiskutiran utjecaj različitih relevantnih aspekata primijenjenih metoda, uzimajući pri tome u obzir obje razine (globalnu i lokalnu) odziva razmatranih nosivih konstrukcija.

Ključne riječi: *analiza progresivnog kolapsa, granična nosivost, nelinearna metoda konačnih elemenata, Smithova metoda, tankostjeni kutijasti nosač*

1 Introduction

Generally, structural collapse event is synonymous to structural ultimate limit state assumed when structural capability to resist imposed structural loading is completely depleted. Since considered monotonous thin-walled structures are comprised of prismatic longitudinal segments segregated by transverse framing (perpendicular to longitudinal structural elements), various feasible global structural collapse modes can be characterized as longitudinal and/or transverse, pending depletion of longitudinal and/or transverse structural members load carrying capacity. Generally, longitudinal and transverse global collapse is not independent, since longitudinal collapse can enclose one or more transverse frames, i.e. two or more longitudinal structural segments. Consequently, a lot of various feasible global collapse scenarios should be considered in detail by ultimate limit state analysis, which is very time consuming and therefore not easily accomplishable within limited timeframe available for the structural concept design synthesis (structural safety as design constraint and/or design objective [1]). Therefore, additional design constraints regarding geometrical and material properties of transverse framing are introduced into structural design process, in order to ensure imminent occurrence of inter-frame collapse of longitudinal structure prior to occurrence of any more complex collapse mode which might encompass larger structural portion (more than one longitudinal structural segment). This enables decoupled consideration of longitudinal and transverse global structural collapse and enables execution of progressive collapse analyses separately for each individual longitudinal structural segment.

Longitudinal structural collapse of various realistic thin-walled structures (e.g. ship, airplane, etc.) is governed and influenced mostly by the imposed flexural loads. Therefore, longitudinal load-capacity is commonly expressed in terms of the maximum attainable moment of the internal longitudinal forces acting at the transverse cross section of the critical longitudinal structural segment. If intensity of the imposed flexural load exceeds this ultimate load-capacity level, occurrence of inter-frame collapse is considered to be imminent, meaning that flexural stiffness of the critical longitudinal segment has been reduced to the ultimate level due to progressive load-capacity depletion of longitudinal structural members. Thereby, progressive collapse of longitudinal structural members can be induced either by yielding or various feasible buckling modes. Longitudinal structural segment whose longitudinal position coincides with the longitudinal position of the maximum bending moment is commonly identified as the critical segment and the change of its load-carrying ability during progressive increase of flexural load intensity is evaluated. Effects of other moments (bending and torsion), transverse forces and local loads (pressure) are usually neglected thereby. However, their relevance and means of proper incorporation into progressive collapse analysis are subjects addressed by past [2-3] and contemporary work of the co-authors as well as other researchers worldwide (e.g. [4-5]).

1.1 Incremental-iterative progressive collapse analysis method (Smith's approach)

Imminent occurrence of inter-frame collapse prior to any other feasible global collapse mode ensures that global structural behaviour of the complex monotonous thin-walled structures submitted to flexure can be idealized in accordance with the beam bending theory during the whole collapse process. This implication represents fundamental premise of the Smith's method [6], which is considered to be first among established progressive collapse analysis methods that incorporate more sophisticated consideration of structural collapse sequence and structural post-critical response of structural elements.

Development of the original method subsequently stimulated proposition of various methods based on Smith's approach (e.g. [7-9]), where some incorporate even further simplifications of the original approach (e.g. [10-12]). In shipbuilding field, rules of many classification societies (and their associations [13-14]) prescribe utilization of incremental-iterative procedures based on Smith's approach for the evaluation of longitudinal ultimate capacity during structural design synthesis. Within the framework of this paper, IACS incremental-iterative progressive collapse analysis method is employed, as previously implemented within OCTOPUS [15] software application, where structural model definition is performed using MAESTRO [16] software application.

1.2 Geometrically and materially nonlinear finite element analysis

For the purposes of ultimate limit state evaluation the most accurate results can be obtained by utilization of the finite element method to perform materially and geometrically nonlinear (NLFEM) analysis of the entire three-dimensional (discretized) structural model, in order to simulate and evaluate nonlinear structural response for various loading levels. However, obtained results depend significantly on correctness of employed structural description and idealization techniques (geometrical and material properties) and boundary conditions (loads and displacement constraints). Although consideration of the complete structural model is always recommendable, available computing and pre/post-processing timeframe often necessitates resortion to partial structural models, where sensitivity of results to idealization of realistic boundary conditions is even more pronounced. Furthermore, employed material models should enable accurate definition of stress to strain relationships during pre-collapse, collapse, and post-collapse regime, while the effect of all relevant initial structural imperfections should be accounted for appropriately, since they can have considerable influence on calculated ultimate load-capacity.

All previously mentioned aspects of NLFEM analysis application considerably limit its utilization for the purpose of structural ultimate load capacity determination within the iterative loop of the concept design synthesis of complex thin-walled structures. Consequently, utilization of NLFEM analysis in the considered context is reduced mostly to the analyses of partial models for the purpose of alternative analysis methods verification (e.g. [17-19]), or to scarce analyses of complete and detailed models in order to reconstruct circumstances and identify causes of real structural collapse events occurred during exploitation of the structure (e.g. [20]). NLFEM analysis is often utilized for derivation and verification of various simplified formulations of elasto-plastic response of structural members (e.g. [21-24]) imposed with various types of pure or combined loads.

All NLFEM analyses performed herein are executed using FEMAP/NX Nastran [25] software application and considered models are discretized using two-dimensional isoparametric finite elements with four (CQUAD4) or (very seldom) three (CTRIA3) nodes. Material nonlinearity is idealized by elasto-plastic (bi-linear) material model disregarding strain hardening, while the employed yield function is expressed in terms of the HMH yield criterion. The Newton-Raphson (unmodified) method was employed as utilized strategy for all solutions of nonlinear stiffness equations.

1.3 Idealization of initial structural imperfections

All metal structures assembled by welding are characterized by imminent presence of initial structural imperfections (initial distortions and residual stresses).

Although the presence of residual stresses can significantly influence structural load capacity, due to complexity of proper idealizations, significant uncertainties regarding proper

description of geometric and material properties of structural regions imposed with residual stresses, and number of relevant technological factors (material type; position, size and type of weld; welding sequence), the influence of residual stresses is often omitted in NLFEM analysis of complex thin-walled structures. Overview of the current practice regarding their proper incorporation into ultimate limit state analysis of structural members might be found in [26-27]. Although IACS method does not support explicit introduction of residual stress effects, their influence might be approximated and introduced indirectly through appropriate change of discrete structural elements material yield stress (e.g. [28]). However, effects of residual stresses are not considered within the scope of work presented in this paper.

Since the shape and intensity of initial distortions (IDs) can significantly influence buckling of structural members loaded in compression, the effects of IDs are commonly incorporated into ultimate load-capacity analysis, regardless of the method employed. While IACS method considers the effect of IDs implicitly within employed load − end shortening curves or average stress − average strain curves (further in the text: $\sigma_{xA} - \varepsilon_{xA}$ curves) (effective breadths of plating and/or effective stiffener web heights are formulated with respect to average intensity level of IDs), utilization of IDs within the scope of NLFEM analysis requires more explicit approach. Commonly, discretized model's node positions are dislocated in accordance with the approach based on consideration of three various buckling modes of structural elements [26]. The final shape of imposed IDs is obtained by superposition of all three types of IDs (see Figure 1), idealized by periodic functions based on Fourier series, while amplitudes of IDs can be determined according to various formulations given by Smith [29] or classification societies. Smith's formulation is commonly preferred by contemporary researchers since it represents more universal idealization, more convenient for various plate thicknesses.
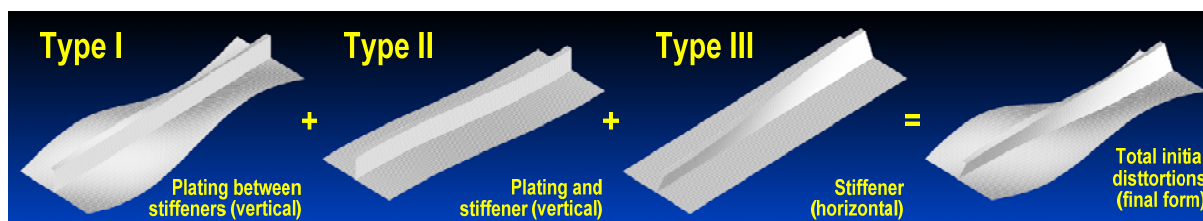

Figure 1 **Superposition of different types of geometric imperfections for plate-stiffener combination**
Slika 1 **Superpozicija različitih tipova IGO za model ukrepe sa sunosivom širinom oplate**

2 Definition and modelling of considered stiffened box-girder structures

This paper considers ultimate limit state of monotonous stiffened box-girders submitted to extreme pure bending (sag), whose ultimate (longitudinal) load-capacity has been investigated experimentally [30]. Geometrical and material properties of considered structures (denoted as P1, P2 and P3) are given by Table 1 through Table 3.

Table 1 **Structural geometry and material characteristics of the model P1**
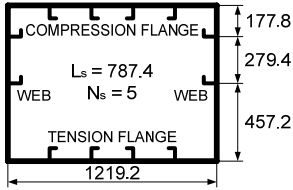Tablica 1 **Geometrijske i materijalne značajke komponenti modela P1**

Structural component	Nominal dimensions [mm]	σ_Y [N/mm^2]	E [N/mm^2]
Compression flange pl.	4.76	298	208000
Tension flange pl.	4.76	298	208000
Web plating	3.18	212	216000
Longitudinal stiffeners	L 50.8x4.76 / 15.88x4.76	276	192000
Transverse framing	L 76.2x6.35 / 50.8x6.35	310	196000

Compression flange geometry: 177.8, 279.4, 457.2, width 1219.2, $L_s = 787.4$, $N_s = 5$, WEB, TENSION FLANGE

Table 2 **Structural geometry and material characteristics of the model P2**
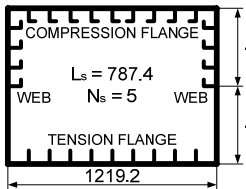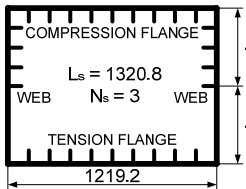Tablica 2 **Geometrijske i materijalne značajke komponenti modela P2**

Structural component	Nominal dimensions [mm]	σ_Y [N/mm^2]	E [N/mm^2]
Compression flange pl.	4.76	221	207000
Tension flange pl.	4.76	216	208000
Web plating	4.76	281	215000
Longitudinal stiffeners (comp. flange and webs)	L 50.8x4.76 / 15.88x4.76	287	199000
Longitudinal stiffeners (tension flange)	FB 50.8x6.35	304	207000
Transverse framing	L 101.6x6.35 / 63.5x6.35	304	201000

Geometry: COMPRESSION FLANGE, 457.2, $L_s = 787.4$, $N_s = 5$, WEB, 457.2, TENSION FLANGE, 1219.2

Table 3 **Structural geometry and material characteristics of the model P3**
Tablica 3 **Geometrijske i materijalne značajke komponenti modela P3**

Structural component	Nominal dimensions [mm]	σ_Y [N/mm^2]	E [N/mm^2]
Compression flange pl.	4.76	221	207000
Tension flange pl.	4.76	216	208000
Web plating	4.76	281	215000
Longitudinal stiffeners (comp. flange and webs)	L 50.8x4.76 / 15.88x4.76	287	199000
Longitudinal stiffeners (tension flange)	FB 50.8x6.35	304	207000
Transverse framing	L 101.6x6.35 / 63.5x6.35	304	201000

Geometry: COMPRESSION FLANGE, 457.2, $L_s = 1320.8$, $N_s = 3$, WEB, 457.2, TENSION FLANGE, 1219.2

Among them, the structure P1 is of substantial significance, since extensive and detailed measurements of compressive flange plating IDs were performed (see Figure 2). Although modelling of compressive flange plating according to detailed ID description adds considerably to the complexity of overall NLFEM model generation, this explicit approach enables accurate geometry idealization of the most (compressively) loaded portion of the structure P1, which positively affects accuracy of the analysis results. Due to the absence of ID data regarding remaining structural parts, the co-authors approximated them according to the previously mentioned approach based on Fourier series, where ID amplitudes are determined for average ID level according to Smith's formulation.
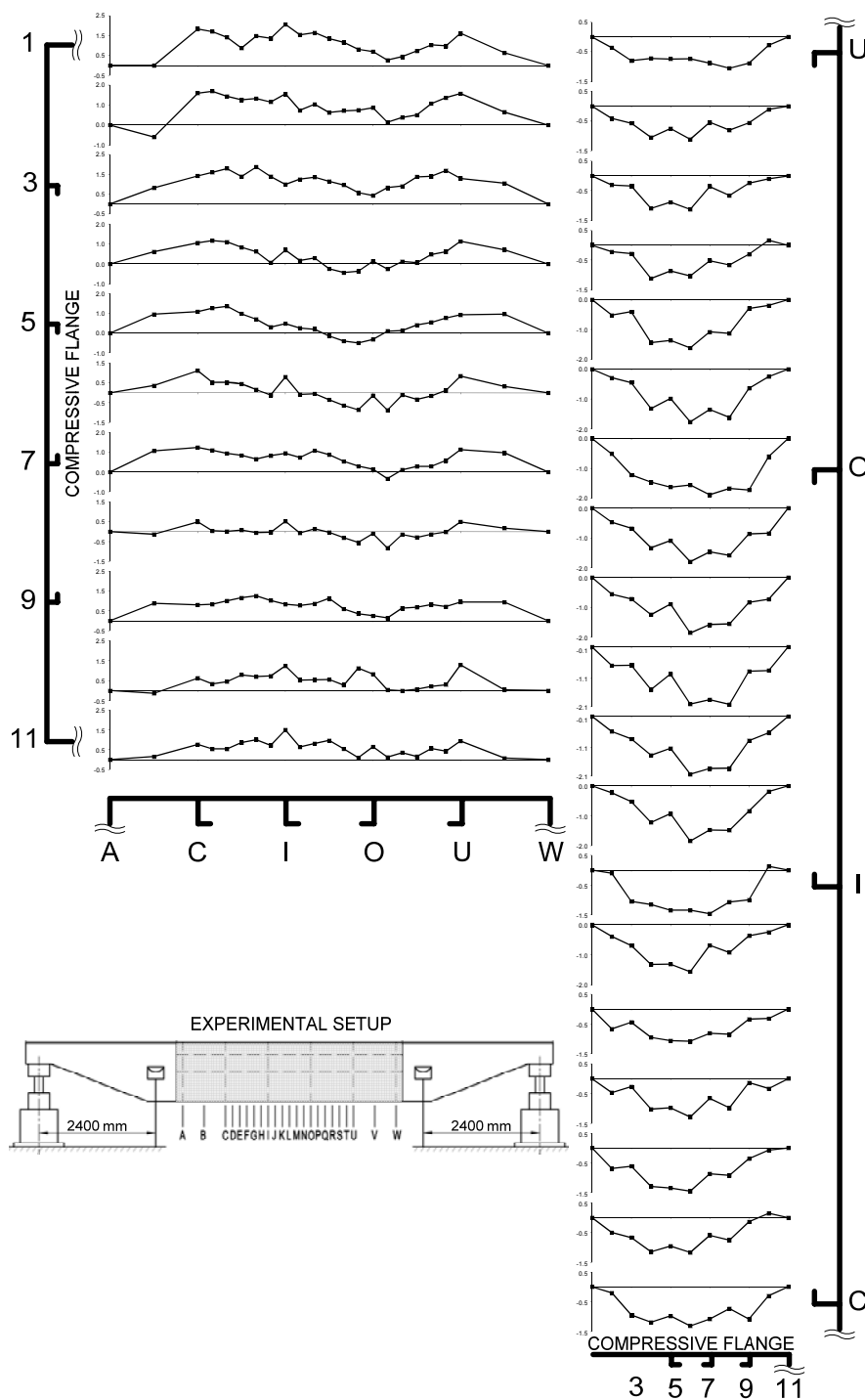
Figure 2 **Measured lateral and transverse IDs for compressive flange of the structure P1**
Slika 2 **Mjerena lateralna i poprečna inicijalna geometrijska odstupanja tlačnog pojasa konstrukcije P1**

2.1 Mesh convergence study for NLFEM model of structure P1

Generation of properly discretized NLFEM model necessitates rational determination of appropriate finite element mesh density. For this purpose a mesh convergence study is performed, where one compressive flange stiffener-plate combination (SPC) is considered to be sufficiently representative portion of the critical part of the structure P1. In accordance with guidelines given by relevant literature (e.g. [26]) and similar work performed by other researchers (e.g. [22], [31-32]), the considered NLFEM model longitudinally encloses two

442

half-spans between transverse framing, while encompassing two half-breadths between stiffeners transversely (Table 4).

Table 4 **Boundary conditions (convergence study model)**
Tablica 4 **Mjesta zadavanja rubnih uvjeta (model korišten za studiju konvergencije rješenja)**

	Node location	Degrees of freedom					
		Tx	Ty	Tz	Rx	Ry	Rz
	A1-A3], [A2-A3 , [A3-A4], [A4-A5], C1-C3], [C2-C3 , [C3-C4], [C4-C5].	0*	1	1	1	0	0
	A1-B1 , B1-C1 , A2-B2 , B2-C2 .	1	0	1	0	1	0
	B1-B3 , B2-B3 , B4-B5].	1	1	0	1	1	1
	B3-B4 .	1	0	1	1	1	1
	A1, A2.	0*	0	1	0	0	0
	C1, C2.	0	0	1	0	0	0
	B1, B2.	1	0	0	0	1	0
	B3, B4.	1	0	0	1	1	1

0   Disabled.
1   Enabled.
*   All nodes of transverse section "A" are imposed with the same loading (displacement in negative direction of x-axis), where all these nodes have this translation constrained solely due to employed software application pre-processing rule requirements.

Transverse frame is not modelled explicitly and its effect is idealized by boundary conditions imposed on nodes of transverse section "B". Considering loading imposed on compressive flange during sagging of the structure P1, the considered SPC model is uni-axially compressed by uniform longitudinal displacement imposed on nodes of transverse section "A", although enforced boundary conditions induce occurrence of the biaxial stress state due to the Poisson effect. Intensity of imposed longitudinal displacement is selected so as to enable enclosure of pre-collapse, collapse, and post-collapse response regime of the considered model by performed NLFEM analyses.

Mesh convergence study is performed for four different ID levels (slight, severe and average according to Smith, and average according to classification society rules) in order to evaluate the influence of their intensity upon obtained results. The largest among the measured magnitudes of IDs (see Figure 2) are: 2.04 mm (for plating lateral/vertical IDs) and 2.06 mm (for plating transverse/horizontal IDs), while the calculated amplitudes of idealized IDs (for plating lateral/vertical IDs; Type I) used for mesh convergence study models are: 0.33 mm (slight ID level according to Smith), 1.33 mm (average ID level according to Smith), 1.22 mm (average ID level according to classification societies), 4.00 mm (severe ID level according to Smith). Amplitudes for additional transverse (Type II) and stiffener lateral (Type III) IDs are identical for all ID intensity levels and both read 1.18 mm. Eight levels of finite element mesh refinements are employed for each ID level, resulting in total of 32 models considered. Table 5 gives characteristics of various mesh densities considered by the performed mesh convergence study and while designations are given for meshes with idealized IDs of average (Smith) level, the same mesh characteristics apply for meshes with other considered ID levels.

Table 5 **Designations and characteristics of various models considered by mesh convergence study**
Tablica 5 **Oznake i značajke različitih modela obuhvaćenih studijom konvergencije rješenja**

ID Amplitude level	Mesh designation	Number of finite elements					Number of nodes	Number of DoFs
		P	W	F	L	T		
	Mesh2B-1	4	2	1	12	84	104	624
	Mesh2B-2	8	3	1	24	288	325	1950
	Mesh2B-3	12	4	1	36	612	666	3996
Average (Smith)	Mesh2B-4	12	5	2	36	684	740	4440
	Mesh2B-5	16	6	2	48	1152	1225	7350
	Mesh2B-6	20	7	2	60	1740	1830	10980
	Mesh2B-7	24	8	3	72	2520	2628	15768
	Mesh2B-8	28	9	3	84	3360	3485	20910

DoF	Degree of freedom;
P	Breadth of plating between stiffeners;
W	Stiffener web height;
F	Stiffener breadth of flange;
L	Length between transverse frames;
T	Total.

Figure 1 illustrates the shapes of the previously mentioned ID types (regardless of amplitude intensity) for the considered models, as well as the final ID form obtained by their superposition. Figure 3 depicts (normalized) $\sigma_{xA} - \varepsilon_{xA}$ curves obtained by NLFEM analyses performed for eight different mesh densities with average ID level (according to Smith) imposed. A qualitatively identical trend characterizes the results obtained for all other considered ID levels and their formulations. Figure 4 gives the obtained values of: normalized ultimate strength (maximum values on curves given by Figure 3), normalized post-collapse strength (at $\varepsilon_{xA} = 1.1\varepsilon_Y$), and vertical nodal displacement at point A2, for the considered mesh densities (represented by total number of degrees of freedom).
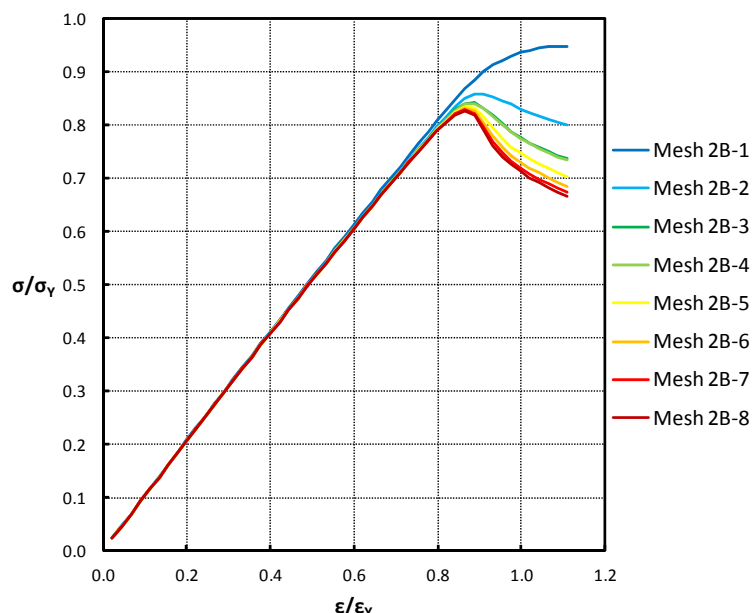

Figure 3 **Normalized $\sigma_{xA} - \varepsilon_{xA}$ curves**
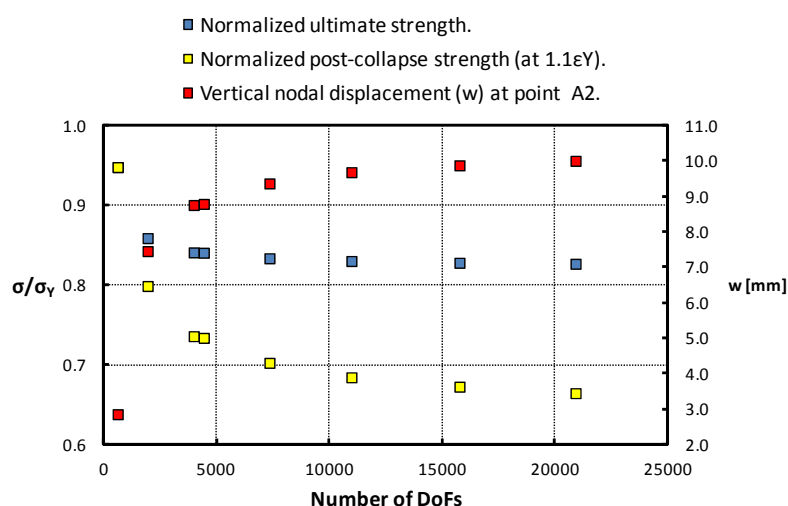Slika 3 **Normalizirane $\sigma_{xA} - \varepsilon_{xA}$ krivulje**

Figure 4 **Comparison of relevant results**
Slika 4 **Usporedba različitih rješenja**

Common practice regarding mesh convergence study (performed within context of the considered problem) usually considers stabilization of obtained ultimate strength values as sole criterion for appropriate mesh density selection. However, Figure 3 and Figure 4 indicate and exemplify relatively rapid stabilization of ultimate strength values (already after the fourth mesh refinement) and an identical trend is characteristic for all employed ID levels.
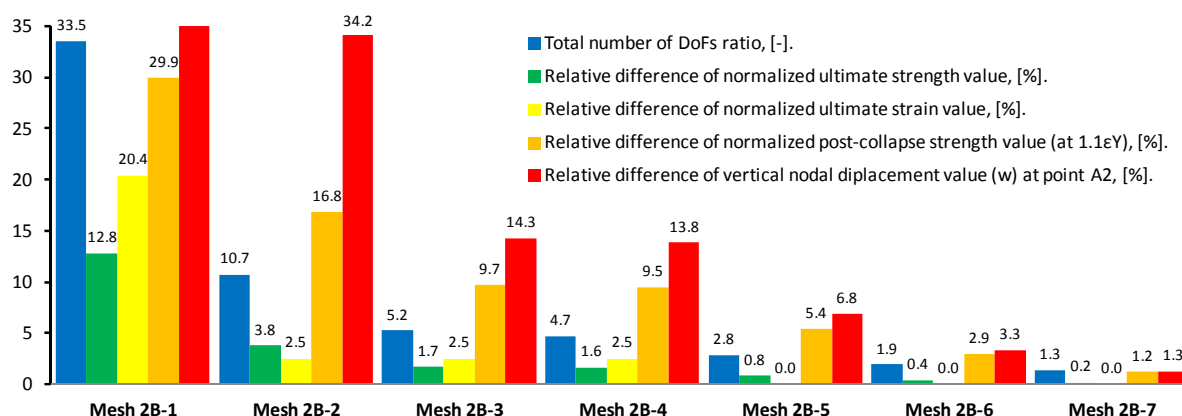
Figure 5 **Solution convergence for average level of imperfections (Smith) with respect to Mesh 2B-8 solutions**
Slika 5 **Konvergencija rješenja za srednju razinu (Smith) inicijalnih geometrijskih odstupanja s obzirom na rješenja dobivena za Mrežu 2B-8**

Furthermore, it should also be noted that post-collapse strength changes significantly for various mesh densities, i.e. that solution stabilizes only at very fine mesh densities. Since the structural members will be characterized by various levels of load-capacity at ultimate limit state of the considered overall structure (in general case some of them will be in pre-collapse, some in collapse, and some in post-collapse response regime), it is very important to describe accurately the post-collapse response of structural members. Disregard for description quality of structural members post-collapse response in the process of rational determination of appropriate mesh density for the complete structure can result in overly optimistic structural load-capacity levels before, during, and especially after structural collapse regime. Therefore, convergence of post-collapse strength (at $\varepsilon_{xA} = 1.1\varepsilon_Y$), ultimate deformation, and maximum vertical nodal displacement (at point A2) is also considered during selection of appropriate mesh density. Figure 5 gives a concise overview of convergence for all previously mentioned

445

solutions (for average ID level according to Smith), as well as change in the number of degrees of freedom, all with respect to the solutions and the number of degrees of freedom obtained for the finest considered mesh density.

The obtained results (for all considered ID levels) stimulate selection of the sixth mesh refinement (Mesh 2B-6, Figure 5) as the reference mesh density employed for overall discretization of the structure P1, since the values of all considered solutions (irrespective of employed ID level) obtained for this mesh density diverge acceptably from the most accurate set of considered solutions eight levels of mesh refinement at almost half of the employed degrees of freedom. Selection of finer mesh densities would result in a considerably higher total number of degrees of freedom with relatively insignificant accuracy improvement. On the other hand, selection of coarser mesh densities would significantly reduce the total number of degrees of freedom, but with significant and unacceptable accuracy penalties regarding some solutions (post-collapse strength and nodal displacements).

2.2 NLFEM model of structure P1

Half-span NLFEM model of the structure P1 is discretized by total of 78640 finite elements (78883 nodes or 473298 degrees of freedom). All nodes belonging to longitudinal structure (whole structure without transverse framing) are dislocated according to the previously mentioned ID idealization approach (for average ID level according to Smith), except compressive flange nodes which are dislocated according to the results of explicit ID measurements. Imposed rotation of the transverse section "A" about y-axis (Table 6) is progressively incremented (0 rad to 0.0075 rad) during NLFEM analysis, in order to simulate pure symmetric bending (sag), as imposed during experimental testing. Loading is imposed on the node coinciding with point A2 and is transmitted onto all remaining nodes of transverse section "A" by means of rigid connections (RBE2 element, [25]). Since the transverse section "A" coincides with the welded joint between the experimentally tested box-girder and the (very rigid) loading arm (of the experimental setup) and since the transverse section "B" belongs to the plane of (loading and geometrical) symmetry of the structure P1, boundary conditions are imposed as described by Table 6.

Table 6 **Loads and boundary conditions for NLFEM model of the P1structure**
Tablica 6 **Mjesta zadavanja ograničenja pomaka i opterećenja za diskretizirani NLMKE model konstrukcije P1**
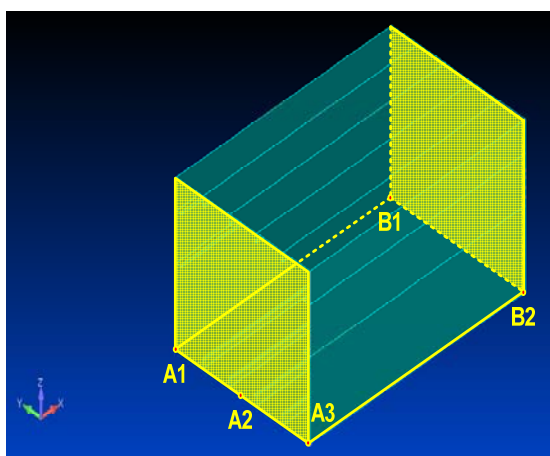
Node location	Degrees of freedom					
	Tx	Ty	Tz	Rx	Ry	Rz
A2	1	0	0	0	0*	0
Section "B"	0	1	1	1	0	0

0   Disabled.
1   Enabled.
*   Load (rotation about y-axis) is imposed on node coinciding with point A2 and transmitted onto all remaining nodes of section "A" by means of rigid connections. This DoF is constrained solely due to employed software application pre-processing rule requirements.

2.3 Progressive collapse analysis models of considered structures

Figure 6 illustrates models of longitudinal segments of the structures P1, P2 and P3 (generated by MAESTRO software application), which are used for discretization according to the employed IACS incremental-iterative progressive collapse analysis method (implemented within OCTOPUS software application).
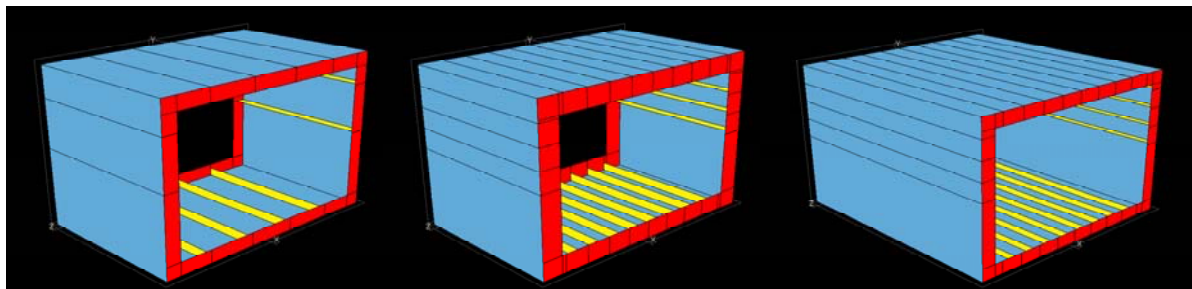

Figure 6 **One-bay model (span of one web frame spacing) of the P1, P2 and P3 structures**
Slika 6 **Modeli uzdužnog segmenta (uzdužni raspon između okvirnih nosača) konstrukcija P1, P2 i P3.**

3 Comparison of obtained results

3.1 IACS method vs. experimental testing of structures P1, P2 and P3

Figure 7 depicts ultimate load-capacity results for the structure P1 submitted to pure symmetric bending (sag), obtained by the employed IACS method (M-κ diagram) and experimental testing. The results of experimental testing are published in terms of instantaneous load versus average transverse (vertical) displacement (w_M) of various points on the mid-span of structural webs (sides). Therefore, vertical displacement of the sectional centroid (neutral axis), relevant for proper calculation of corresponding physical curvature, remains unknown. Consequently, the obtained results cannot be displayed in the same form and/or within the same diagram. Analogous to the previous description, Figure 8 and Figure 9 are displaying the results obtained for the structures P2 and P3 respectively.
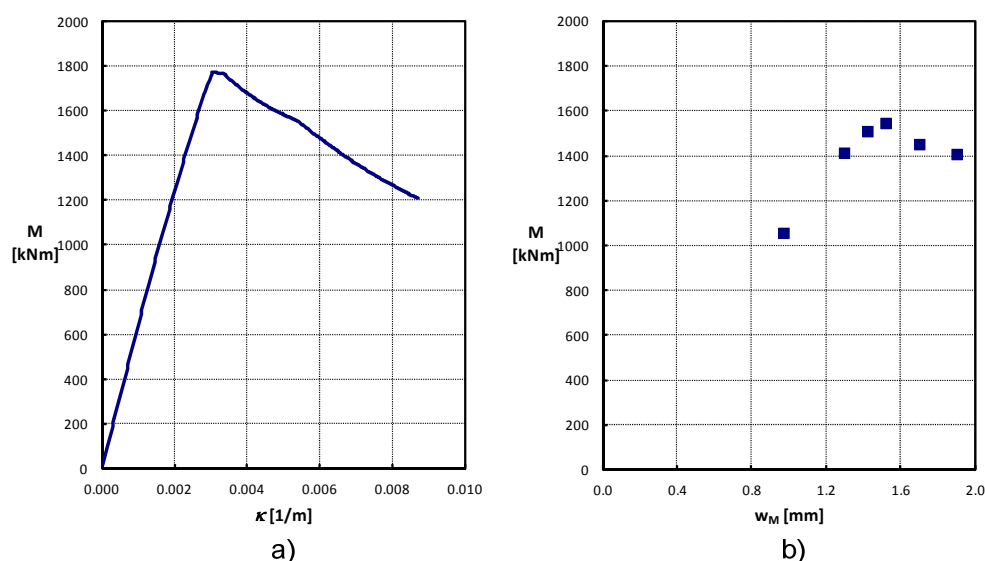

a)   b)

Figure 7 **Ultimate strength analysis results for the P1 structure: a) IACS method; b) experimental testing**
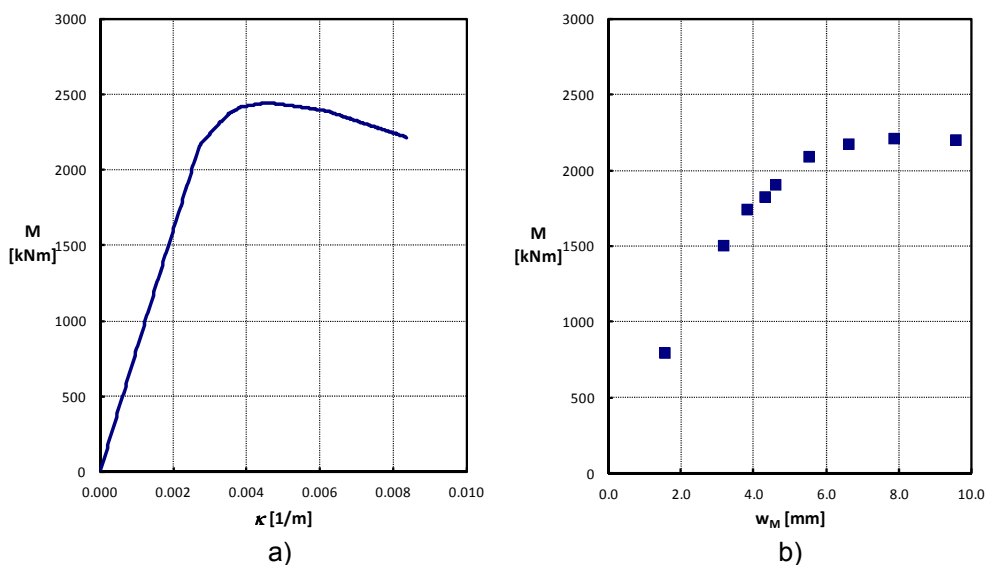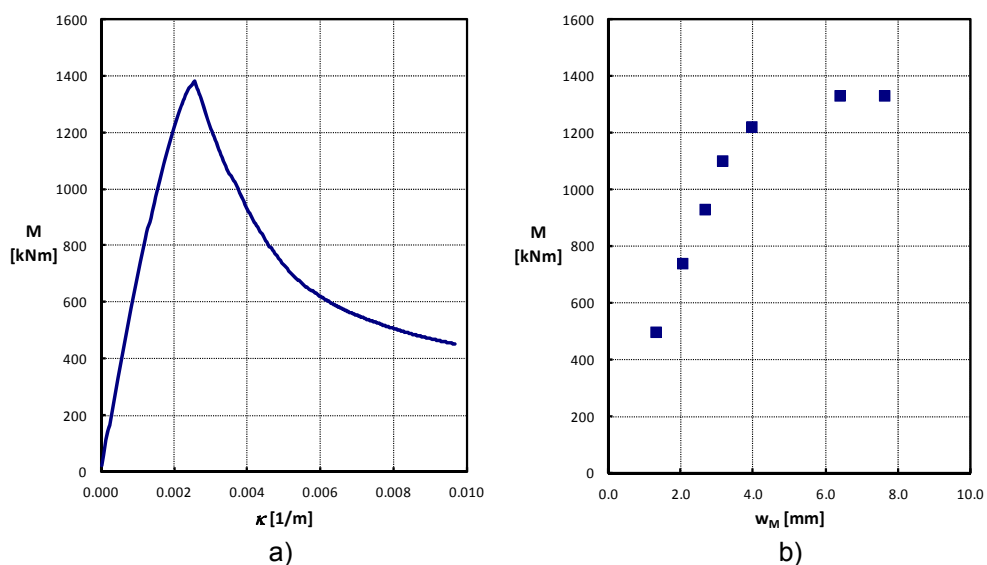Slika 7 **Rezultati analize granične nosivosti konstrukcije P1: a) IACS-ova metoda; b) eksperimentalno ispitivanje**

Figure 8 **Ultimate strength analysis results for the P2 structure: a) IACS method; b) experimental testing**
Slika 8 **Rezultati analize granične nosivosti konstrukcije P2 a) IACS-ova metoda; b) eksperimentalno ispitivanje**

Figure 9 **Ultimate strength analysis results for the P3 structure: a) IACS method; b) experimental testing**
Slika 9 **Rezultati analize granične nosivosti konstrukcije P3: a) IACS-ova metoda; b) eksperimentalno ispitivanje**

Table 7 **Comparison of the obtained and experimental results**
Tablica 7 **Usporedba dobivenih rezultata u odnosu na eksperimentalne**

| Structural designation | Ultimate bending moment M_U [kNm] | | Relative difference* |
	Experiment M_{UE}	IACS method M_{UI}	
P1	1546.7	1771.6	-12.69 %
P2	2214.1	2444.4	-9.42 %
P3	1331.6	1379.6	3.48 %

*	Relative difference is calculated as: % = $(M_{UE}–M_{UI})/M_{UI}·100$;
M_{UE}	Ultimate bending moment determined experimentally;
M_{UI}	Ultimate bending moment determined by IACS method;

Table 7 comparatively gives the ultimate bending moment values determined experimentally and by IACS method. Relatively significant discrepancy of the results obtained for the structures P1 and P2 is induced by utilized $\sigma_{xA} - \varepsilon_{xA}$ curves and discretization rules employed by IACS method. Namely, critical portion (compressive flange) of the analyzed structures is discretized (for the most part) as a set of thin-walled beam-columns. The identified collapse mode for those discrete structural elements in all three structures is beam-column buckling, described by the corresponding $\sigma_{xA} - \varepsilon_{xA}$ curve. In the case of P1 structure, the compressive flange is characterized by a relatively high plate (between stiffeners) slenderness and a relatively low aspect ratio. Hence, the acting collapse mode should be dominated and governed by the collapse of the plating, not the stiffeners (with attached breadth of plating). In the case of P2 structure, twofold number of stiffeners, lower plate slenderness and higher aspect ratio result in better collapse response description of the critical structural portion and the discrepancy of obtained results is therefore lower. In the case of P3 structure, a large number of long stiffeners (high unsupported length) along with other geometrical and material characteristics of compressed structural portion stimulate dominance of beam-column type of collapse, resulting consequently in very good agreement of obtained results.

3.2 IACS prescribed vs. NLFEM derived $\sigma_{xA} - \varepsilon_{xA}$ curves for compressively loaded discrete structural elements of structure P1

The previous discussion implies that the existing IACS $\sigma_{xA} - \varepsilon_{xA}$ curves employed within context of current discretization rules prescribed by contemporary IACS method are not universally adequate for arbitrary stiffened panel configuration, i.e. that their utilization in the case of stiffened panels with a slender plating (between stiffeners) and a relatively small number of stiffeners will not provide sufficiently accurate results. In order to minimize foul effect of the employed IACS $\sigma_{xA} - \varepsilon_{xA}$ curves on overall results, for all discrete structural elements of P1 structure (loaded in compression during progressive collapse analysis), a new $\sigma_{xA} - \varepsilon_{xA}$ curve is derived using NLFEM analysis. For this purpose, discretized (in reference mesh density) NLFEM models of considered discrete structural members (SPCs, hard corners, transversely stiffened plating) are imposed with average ID amplitude level (according to Smith) and loaded in uniform uni-axial (longitudinal) compression. In order to enable practical inclusion of derived $\sigma_{xA} - \varepsilon_{xA}$ curves into the framework of IACS method, B-spline approximation [33] using existing Fortran subroutines of FITPACK [34] public on-line library is employed. Boundary conditions identical to those used for mesh convergence study (Table 4) were employed for derivation of NLFEM $\sigma_{xA} - \varepsilon_{xA}$ curves for SPC models of box-girder web (side) and compressive flange. Location and description of boundary conditions imposed on models of hard corners and transversely stiffened plating are given in Table 8 and Table 9 respectively. Figure 10 comparatively illustrates the derived NLFEM and IACS $\sigma_{xA} - \varepsilon_{xA}$ curves for some of the considered discrete structural elements. Considerable discrepancy among the curves might be observed for the majority of the considered discrete structural members.

Table 8 **Boundary conditions (hard corner model)**
Tablica 8 **Opis čvornih ograničenja pomaka (element krutog kuta)**

Node location	Tx	Ty	Tz	Rx	Ry	Rz
A1-A2], [A2-A3 , C1-C2], [C2-C3 .	0*	1	1	1	0	0
A1-B1 , B1-C1 .	1	0	1	0	1	0
A3-B3 , B3-C3 .	1	1	0	0	1	0
B1-B2 .	1	1	0	1	1	1
B2-B3 .	1	0	1	1	1	1
B2.	1	0	0	1	1	1
B1, B3.	1	0	0	0	1	0
A1, C1.	0*	0	1	0	0	0
A3, C3.	0*	1	0	0	0	0

(Degrees of freedom)

0	Disabled.
1	Enabled.
*	All nodes of transverse section "A" are imposed with the same loading (displacement in positive direction of *x*-axis), where all these nodes have this translation constrained solely due to employed software application pre-processing rule requirements.

Table 9 **Boundary conditions (transversely stiffened plate model)**
Tablica 9 **Opis čvornih ograničenja pomaka (element poprečno orebrene oplate)**

Node location	Tx	Ty	Tz	Rx	Ry	Rz
A1-A2 , C1-C2 .	0*	1	1	1	0	0
A1-B1], [B1-C1 , A2-B2], [B2-C2 .	1	0	0	0	1	0
B1-B2	1	1	0	1	1	1
A1, A2.	0*	0	0	0	0	0
C1, C2.	0	0	0	0	0	0

(Degrees of freedom)

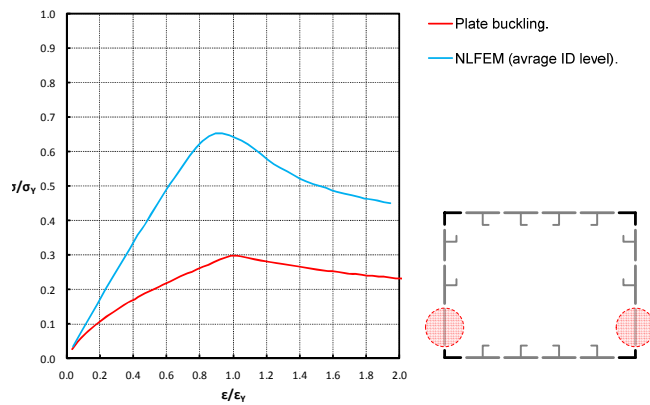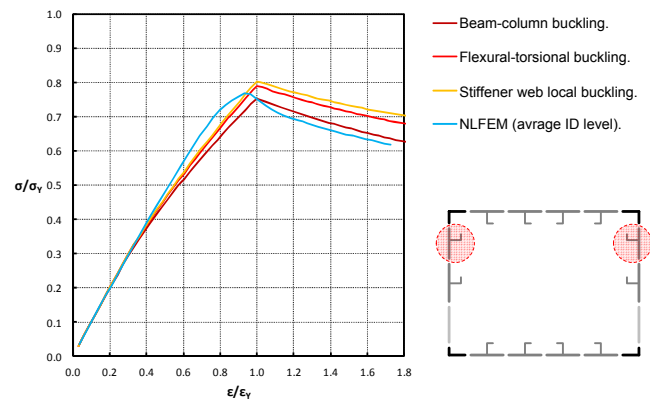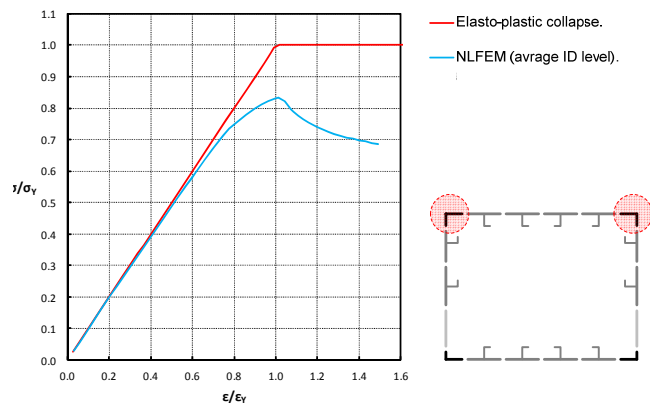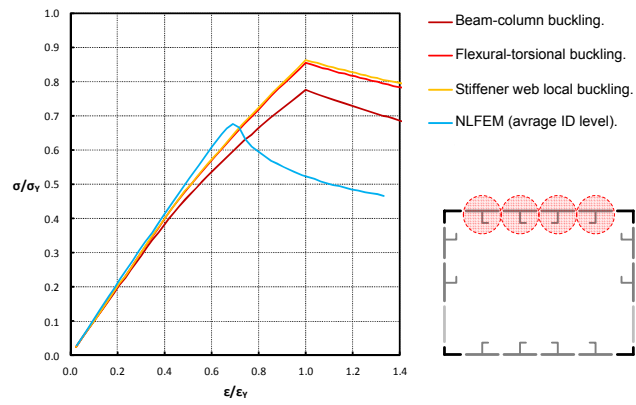| 0	Disabled.
1	Enabled.
*	All nodes of transverse section "A" are imposed with the same loading (displacement in positive direction of *x*-axis), where all these nodes have this translation constrained solely due to employed software application pre-processing rule requirements.

Figure 10 **Comparison of IACS and NLFEM $\sigma_{xA} - \varepsilon_{xA}$ curves for various discrete elements of P1 structure**
Slika 10 **Usporedba IACS i NLMKE $\sigma_{xA} - \varepsilon_{xA}$ krivulja za različite diskretne sastavne elemente konstrukcije P1**

451

3.3 Ultimate load-capacity results for structure P1

Figure 11 gives comparison of ultimate load-capacity analysis results obtained for structure P1 (submitted to pure symmetric bending) by various considered numerical simulation methods. Considerable discrepancy (22.18 %) might be observed among ultimate load-capacity values obtained by IACS method and alternative progressive collapse analysis method (further in the text: alternative PCA method) employing overall framework of IACS method with NLFEM $\sigma_{xA} - \varepsilon_{xA}$ curves. The same figure also illustrates progressive change in the moment of internal longitudinal forces (acting at the mid-span transverse section of P1 structure) for a few characteristic load increments of the NLFEM analysis of the half-span P1 model. Finally, Table 10 gives comparison of the ultimate load-capacity analysis results obtained for P1 structure by various considered numerical simulation methods, where indicated relative differences are calculated with respect to experimental results.
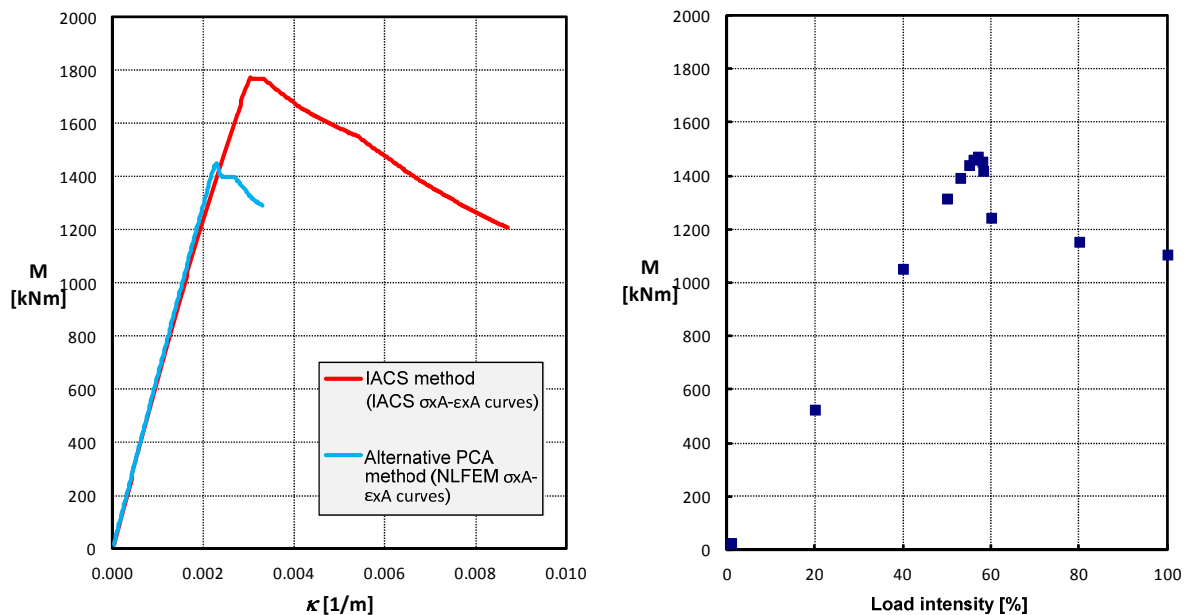

Figure 11 **Ultimate load-capacity analysis results for P1 structure**
Slika 11 **Rezultati analize granične nosivosti konstrukcije P1**

Table 10 **Comparison of the results obtained with respect to experimental testing**
Tablica 10 **Usporedba dobivenih rezultata s obzirom na eksperiment**

Structure P1 progressive collapse analysis method	M_U [kNm]	Relative difference*
Experiment	1546.7	0 %
NLFEM	1472.1	5.07 %
Alternative PCA method (NLFEM curves)	1450.1	6.66 %
IACS method	1771.6	-12.69 %

*   Relative difference is calculated with respect to experimental results: % = $(M_{UE}-M_U)/M_U \cdot 100$;

4 Conclusions

Within the scope of this paper a need for more comprehensive approach regarding mesh convergence study is argumented in the context of NLFEM analysis utilization for complex thin-walled structures ultimate load-capacity assessment and/or for derivation of $\sigma_{xA} - \varepsilon_{xA}$ curves employed by alternative progressive collapse analysis methods. Furthermore, it is

shown that existing IACS $\sigma_{xA} - \varepsilon_{xA}$ curves employed within context of current discretization rules prescribed by contemporary IACS method are not universally adequate for arbitrary stiffened panel configuration, i.e. that their utilization in the case of stiffened panels with slender plating (between stiffeners) and relatively small number of stiffeners will not provide sufficiently accurate results. Comparison of ultimate load-capacity analysis results (obtained for structure P1 by various considered numerical simulation methods) with reference (experimental) results implies that utilization of NLFEM $\sigma_{xA} - \varepsilon_{xA}$ curves can significantly increase the accuracy of the progressive collapse analysis. Additionally, in contrast to the result obtained by utilization of IACS curves, conservative ("on-safe-side") character of the result obtained by utilization of NLFEM curves (with respect to experimental reference) should also be noted. Considering relatively small discrepancy (1.52 %) among the results obtained by alternative PCA method (utilizing NLFEM $\sigma_{xA} - \varepsilon_{xA}$ curves) and NLFEM analysis of the global model, it might be concluded that this approach can represent an efficient alternative to NLFEM analysis for the considered type of structures when submitted to the considered type of loading. In addition to sufficient accuracy, this approach can provide considerable savings in pre-processing and computing time, especially in the case of complex thin-walled structures comprised of a large number of structural members with identical geometrical and material properties (one $\sigma_{xA} - \varepsilon_{xA}$ curve for all identical discrete structural members).

However, residual stresses, not considered in this work, certainly contributed in some extent to the discrepancy of the results obtained by the employed simulation methods and experimental testing. Furthermore, only a limited number of structural configurations were considered by the present study. Hence, the obtained results may be considered as a good measure of IACS method accuracy only when employed for progressive collapse analysis of structures analogous to those considered. Similarly, the applicability of the derived conclusions should be considered in the same manner.

Furthermore, the obtained results suggest that fidelity of the IACS method, when employed within the framework of design procedure (see [1]), is considered sufficient for correct comparison of the design variants with respect to the safety objective (ultimate load-capacity based safety measure). The obtained results show that the applied safety measure, when used in formulation of the design constraints, would certainly satisfy the accuracy required for the concept design phase.

Acknowledgement

References

[1] ŽANIĆ, V., KITAROVIĆ, S., PREBEG, P.: "Safety as objective in multicriterial structural optimization", Proceedings of the 29th International Conference in Ocean, Offshore and Arctic Engineering, Shangai, 2010, p. 899-910.
[2] KITAROVIĆ, S., ANDRIĆ, J., ŽANIĆ, V.: "Extended IACS incremental-iterative method for calculation of hull girder ultimate strength in analysis and design", Advanced Ship Design for Pollution Prevention, Carlos Guedes Soares, Joško Parunov, editor(s). Taylor & Francis Group, London, 2010, p. 103-112.
[3] KITAROVIĆ, S.: "Analysis of longitudinal ultimate load-capacity in concept synthesis of thin-walled structures", Doctoral thesis, University of Zagreb, FMENA, Zagreb, 2012 (in Croatian).

[4] YAO, T., IMAYASU, E., MAENO, Y., FUJII, Y.: "Influence of warping due to vertical shear force on ultimate hull girder strength". Proceedings of the 9th Symposium on Practical Design of Ships and Other Floating Structures, 2004, p. 322-328.

[5] AMLASHI, H.K.K., MOAN, T.: "Ultimate strength analysis of bulk carrier hull girder under alternate hold loading condition, Part 2: Stress distribution in the double bottom and simplified approaches". Marine Structures, Vol.22, 2009, p. 522-544.

[6] SMITH, C.S.: "Influence of local compressive failure on ultimate longitudinal strength of a ship's hull", Proceedings of the International Symposium on Practical Design in Shipbuilding, Tokyo, 1977, p. 73-79.

[7] DOW, R.S.: "A computer program for elasto plastic, large deflection buckling and post buckling of plane frames and stiffened panels", Report AMTE(S) R80762, 1980.

[8] YAO, T., NIKOLOV, P.I.: "Progressive collapse analysis of a ship's hull under longitudinal bending (2nd Report)", Journal of Society of Naval Architects, Vol.172, 1992, p. 437-446.

[9] GORDO, J.M., SOARES, C.G.: "Approximate method to evaluate the hull girder collapse strength", Marine Structures, Vol.9, 1996, p. 449-470.

[10] ADAMCHAK, J.C.: "ULSTR, A program for estimating the collapse moment of ship's hull under longitudinal bending", DTNSRDC Report 82/076, 1982.

[11] HUGHES, O.F.: "Ship structural design - A rationally-based computer-aided optimization approach". The Society of Naval Architects and Marine Engineers, 1988.

[12] RAHMAN, M.K., CHOWDHURY, M.: "Estimation of ultimate longitudinal bending moment of ships and box girders", Journal of Ship Research, Vol.40, 1996, p. 244-257.

[13] …: "Common Structural Rules for Double Hull Oil Tankers", International Association of Classification Societies, London, 2012.

[14] …: "Common Structural Rules for Bulk Carriers", International Association of Classification Societies, London, 2012.

[15] …: "OCTOPUS Software Documentation", University of Zagreb, Faculty of Mechanical Engineering and Naval Architecture, Zagreb, 2009.

[16] …: "MAESTRO Software Documentation", DRS-C3 Advanced Technology Center, Stevenswille, 2010.

[17] SERVIS, D., VOUDOURIS, G., SAMUELIDES, M., PAPANIKOLAOU, A.: Finite element modeling and strength analysis of hold No. 1 of bulk carriers, Marine Structures, Vol.16, No.8, 2003, p. 601-626.

[18] ...: "Nonlinear finite element analysis of hull girder collapse of a tanker", Det Norske Veritas, Technical report No.2004-0505, 2004.

[19] AMLASHI, H.K.K., MOAN, T.: "Ultimate strength analysis of bulk carrier hull girder under alternate hold loading condition - A case study Part 1: Nonlinear finite element modeling and ultimate hull girder capacity", Marine Structures, Vol.21, 2008, p. 327-352.

[20] ...: "Report on the investigation of the structural failure of MSC Napoli, English Channel on 18 January 2007". Marine Accident Investigation Branch, Report No.9/2008, 2008.

[21] PAIK, J.K., KIM, B.J., SEO, J.K.: "Methods for ultimate limit state assessment of ships and ship-shaped offshore structures: Part I – Unstiffened plates", Ocean Engineering, Vol.35, 2008, p. 261-270.

[22] PAIK, J.K., KIM, B.J., SEO, J.K.: "Methods for ultimate limit state assessment of ships and ship-shaped offshore structures: Part II – Stiffened panels", Ocean Engineering, Vol.35, 2008, p. 271-280.

[23] ZHANG, S., KUMAR, P., RUTHERFORD, S.E.: "Ultimate shear strength of plates and stiffened panels", Ships and Offshore Structures, Vol.3, No.2, 2008, p. 105-112.

[24] ZHANG, S., KHAN, I.: "Buckling and ultimate capability of plates and stiffened panels in axial compression", Marine Structures, Vol.22, No.4, 2009, p. 791-808.

[25] …: "FEMAP/NX Nastran Software Documentation", Siemens Product Lifecycle Management Software, 2010.

[26] HUGHES, O.F., PAIK, J.K.: "Ship structural analysis and design", The Society of Naval Architects and Marine Engineers, 2010.

[27] PAIK, J.K., THAYAMBALLI, A.K.: "Ultimate limit state design of steel-plated structures", John Wiley and Sons, 2003.

[28] GORDO, J.M., GUEDES SOARES, C.: "Approximate load shortening curves for stiffened plates under uniaxial compression", Integrity of Offshore Structures – 5, D. Faulkner, M.J. Cowling, A. Incecik, P.K. Das, editor(s). EMAS Warley UK, Glasgow, 1993, p. 189-211.

[29] SMITH, C.S., DAVIDSON, P.C., CHAPMAN, J.C., DOWLING, P.J.: "Strength and stiffness of ship's plating under in-plane compression and tension", Transactions of RINA, Vol.130, 1988, p. 277-296.

[30] DOWLING, P.J., CHATTERJEE, S., FRIEZE, P.A., MOOLANI, F.M.: "Experimental and predicted collapse behaviour of rectangular steel box girders", Proceedings of the International Conference on Steel Box Girder Bridges, Institution of Civil Engineers, London, 1973, p. 77-94.

[31] RUTHERFORD, S.E., CALDWELL, J.B.: "Ultimate longitudinal strength of ships: A case study", SNAME Transactions, Vol.98, 1990, p. 441-471.

[32] ĆORAK, M., PARUNOV, J., TEIXEIRA, A.P., SOARES, C.G.: "Performance of the Common Structural Rules Design Formulations for Ultimate Strength of Uniaxially Loaded Plates and Stiffened Panels", Advanced Ship Design for Pollution Prevention, Carlos Guedes Soares, Joško Parunov, editor(s), Taylor & Francis Group, London, 2010, p. 113-120.

[33] DIERCKX, P.: "Curve and surface fitting with splines", Oxford University Press, 1993.

[34] Available at http://www.netlib.org/dierckx/, 25 January 2013.